Postbuckling of Laminated Composite and Sandwich-Type Plates and Shells: On the Significance of the Fulfillment of Static Interlayer Continuity Conditions

Librescu, L. and Lin, W.
Department of Engineering Science and Mechanics
Virginia Polytechnic Institute and State University
Blacksburg, Virginia 24061-0219, USA

M. DiSciuva and U. Icardi
Department of Aeronautical and Aerospace Engineering
Politecnico di Torino
Torino 10129, Italia

Abstract

Two structural models of multilayer sandwich type structures are presented and used to study their postbuckling response. Whereas in one of the considered structural models the ***kinematic*** continuity at the contact between the contiguous layers and the free traction condition on the outer bounding surfaces are solely satisfied, in the second model, in addition to these conditions also the ***static*** interlaminae continuity requirement is fulfilled.

Comparisons of the postbuckling behavior obtained in the context of the two structural models are presented and pertinent conclusions on the implications of the violation of the static continuity requirement are outlined. In order to study this problem, as a basic pre-requisite, a geometrically non-linear structural model of initially imperfect laminated shells fulfilling both the static and kinematic interlaminae continuity requirements is briefly presented, as well.

Nomenclature

$a_{\alpha\beta}$, $a^{\alpha\beta}$	Covariant and contravariant components of the metric tensor of the undeformed mid-surface σ
$\mathcal{T}, \mathcal{L}, \mathcal{S}, \mathcal{K}, \tilde{b}, \tilde{c}$	Stiffness quantities
$b_{\alpha\beta}$	Curvature tensor of the undeformed mid-surface
$b_{11}(\equiv 1/R_1); b_{22}(\equiv 1/R_2)$	Principal curvatures of σ
$c^{\alpha\beta}$	2-D permutation symbol
D	Flexural stiffness
$e_{\alpha\beta}, e_{\alpha 3}$	Tangential and transverse shear 3-D strain components
E	Young's modulus, tangential to the isotropy surface
$f(x^3)$	Function characterizing the variation of $\sigma^{\alpha 3}$ in the thickness direction
$f_{mn}, \overset{\circ}{f}_{mn}$	The amplitudes in the mode (m,n) of v_3, $\overset{\circ}{v}_3$
$F_\omega(x^\alpha)$	Functions defining the tangential variation of σ^{α^3}
G, G'	Tangential and transverse shear modulus
h	Total thickness of shell/ plate
H	Mean curvature of σ
K^2	Transverse shear correction factor
N_{11}, N_{22}	Edge loads normal to the edges $x_1 = 0$, ℓ_1 and $x_2 = 0, \ell_2$, respectively, positive in compression
ℓ_1, ℓ_2	Length and width of the flat/curved panel
$\tilde{L}_{11}, \tilde{L}_{22}$	Dimensionless compressive edge loads $(\equiv (N_{11}, N_{22})\ell_1^2/\pi^4 D$
L_R	The ratio $\tilde{L}_{22}/\tilde{L}_{11}$
$N^{\alpha\beta}, M^{\alpha\beta}, Q^{\alpha 3}$	Tensors of stress resultants, stress couples and transverse shear stress resultant, respectively

p_3, p_{mn}, Lateral pressure field, its amplitude in the mode (m,n)

$\hat{p}(\equiv p_{11}\ell_1^4/(Dh)$ and the dimensionless amplitude in the mode (1,1), respectively

S^{ij} Second Piola-Kirchhoff stress tensor

t_c, t_f Thickness of the core and of upper or bottom face layers, respectively

v_α, v_3 Tangential and transversal displacaement quantities of the mid-surface of plate/shell

$\overset{\circ}{v}_3$ Initial geometric imperfection

x^i Curvilinear system of normal coordinates

Ψ_1 Airy's potential function and particular solution of Eq. (28), respectively

ϕ Boundary layer solution

λ_m, μ_n $m\pi/\ell_1,\ n\pi/\ell_2$

$\delta(\equiv f_{11}/h), \delta_0(\equiv \overset{\circ}{f}_{11}/h)$ The dimensionless amplitudes of the transverse deflection and of initial geometric imperfection, respectively

δ^i_j Kronecker delta

Δ_1 The end-shortening in the x_1 direction

ν, ν' Poisson's ratios tangential and transversal to the isotropy surface

$(\ )_{,i}$ Partial differentiation with respect to coordinates x^i

$(\ )\|_i, (\ )|_\alpha$ Covariant differentiation with respect to the metric tensor g_{ij} and $a_{\alpha\beta}$, respectively

Introduction

As the concept of high-speed, highly flexible and light structural weight aircraft capable of operating in a hostile flight environment gathers more impetus, the specialists are more and more challenged with a variety of new technical problems involving its design.

Such new problems are generated, among others, by the fact that the advanced supersonic and hypersonic flight vehicles are likely to experience, during their operational life, high temperature and pressure gradients. As a result of these severe environmental conditions, high compressive stresses acting on the edges of the constituent panels are induced. For this reason, the study of the postbuckling behavior of flat/curved structures under complex loading conditions is a matter of considerable importance in the design of supersonic/hypersonic aircraft.

Of great promise toward the successful solution of a number of technical challenges raised by the design of advanced flight vehicles is the ongoing integration of advanced composite material systems. A typical laminated composite structure which was used in aeronautical industry in the past and is of great promise in the design of next generations of high-speed and launch vehicles is the sandwich type construction. In its simplest form the sandwich type constructions can be viewed as a structure composed of two thin, stiff layers (face layers) separated by a thick mid-layer of low density material (core layer), and in a most general form, as a multi-sandwich construction constituted of a number of thin layers interspersed with thick layers constituting the cores.

As the present authors of this article are aware, in the available studies devoted to the modeling of sandwich-type structures the continuity requirement for the interlaminae transverse shear stresses is generally not fulfilled and consequently, the study of the postbuckling of sandwich type structures was performed by violating this requirement.

A number of recent survey papers [1,2] and specialized papers dealing with the linear behavior of laminated composite structures (see Refs. 3-8) reveal that the violation of this requirement can result in unavoidable errors in the accurate response prediction. Moreover, these errors can be even exacerbated in sandwich type structures where the materials of the face layers exhibit large stiffness properties in transverse shear while the core layer features high flexiblities in transverse shear. This feature, resulting in large jumps in transverse shear properties across the interlaminae surfaces, is likely to increase the errors incurred by the violation of the static continuity requirement.

Although the specialized literature contains a number of important contributions related to the foundation of the *linear* theory of laminated composite plates/shells based on the fulfillment of the *interlaminae continuity requirement of transverse shear stresses* (ICSS) (e.g. see Refs. 3, 5, 9-13 for the theory of plates and Refs. 4, 6-8, 14, 15, for the theory of shells), to the best of the authors' knowledge,

an assessment of the implications of the violation of this requirement upon the postbuckling response of sandwich-type structures has not yet been addressed. This absence is certainly due to the fact that such a study requires an adequate geometrically non-linear shell model, which, to the best of the knowledge of these authors was developed in a very few papers only, (see Refs, 11, 13, 15-17). The clarification of this issue constitutes one of the basic topics of this work.

In the study of this problem, a number of non-classical effects having a significant influence on the snap-through phenomenon will be also incorporated and their effects highlighted. Among these, there are the initial geometric imperfections, the in-plane edge restraints and the shell curvature. The implications of the non-fulfillment of the ICSS upon the postbuckling response will be analyzed by comparing the predictions based upon the shell/plate model developed in Refs. 18, 19 with their counterparts obtained in the context of a theory fulfilling this requirement.

Towards the goal of elucidating this problem, as a basic pre-requisite, the basic equations associated with a simple discrete-layer geometrically non-linear shell model fulfilling both the kinematic and static interlaminae continuity requirements will shortly be presented. For the sake of convenience, in the forthcoming developments this model is labelled as Model II while the one violating the ICSS requirement as the Model I.

Notations and Preliminaries

Although the numerical illustrations will be applied to three-layer sandwich-type shells/plates, for the sake of generality, the theory is developed for the case of a symmetrically laminated construction, the constituent material layers featuring monoclinic symmetry properties with respect to the global mid-surface of the structure.

One assumes that the layers are in perfect bond, implying that no slip or debonding between two contiguous layers may occur. The points of the 3-D shell space are referred to a set of curvilinear normal system of coordinates x^i, where x^α $(\alpha = 1, 2)$ denote the tangential coordinates, x^3 $(x^3 \leq |h/2|)$ being the normal coordinate to the reference surface σ selected to coincide with the mid-surface of the mid-layer while h denotes the uniform wall thickness of the structure.

The present study will be accomplished in the context of the shallow shell theory (henceforth abbreviated as the SST).

In light of its underlaying assumptions (see e.g. [20]), we may appropriately consider that

$$\mu_\beta^\alpha \left(\equiv \delta_\beta^\alpha - x^3 b_\beta^\alpha\right) \longrightarrow \delta_\beta^\alpha \quad \text{and} \quad \left(\mu^{-1}\right)_\beta^\alpha \longrightarrow \delta_\beta^\alpha \tag{1a,b}$$

where μ_β^α and its inverse $\left(\mu^{-1}\right)_\beta^\alpha$ play the role of shifters in the space of normal coordinates (see Refs. [21,22]). In Eqs. (1), δ_β^α and b_β^α denote the Kronecker delta and the mixed curvature tensor, respectively. In addition, by virtue of the same assumptions, we may obtain for the SST

$$\begin{aligned} &g^{\alpha\beta} \longrightarrow a^{\alpha\beta},\ g_{\alpha\beta} \longrightarrow a_{\alpha\beta}, \\ &\mu \equiv |\mu_\beta^\alpha| = 1 - 2x^3 H + K(x^3)^2 \longrightarrow 1. \end{aligned} \tag{2a-c}$$

In Eqs. (2), $g^{ij}\,(g_{ij})$ and $a^{\alpha\beta}\,(a_{\alpha\beta})$ denote the contravariant (covariant) space and mid-surface metrics while H and K denote the mean and Gaussian curvatures of σ, respectively.

In the above and forthcoming equations, the usual summation convention for the repeated indices is implied, where the Latin indices range from 1 to 3 while the Greek indices have the range 1,2. In addition, subscript or superscript k in the brackets "<>" accompanying any quantity defining the geometry or mechanical properties of the laminated composite, identifies its affiliation to the kth layer.

Transverse Shear Stress Distribution

In the absence of shear tractions on the outer bounding surfaces of the shell $x^3 = \pm h/2$, the following variation of transverse shear stresses across the thickness of each kth layer is postulated (see Refs. 8,12),

$$\sigma_{<k>}^{\alpha 3}(x^\lambda, x^3) = E_{<k>}^{\alpha 3 \omega 3} f\left(x^3\right) F_\omega\left(x^\lambda\right) + B_{<k>}^\alpha\left(x^\lambda\right). \tag{3}$$

In Eq. (3) $f(x^3)$ is the function characterizing the variation of $\sigma^{\alpha 3}$ across the shell thickness. For the present case, f is represented as an even function in the thickness coordinate in the sense of $f(x^3) = f(-x^3)$, and in order to fulfill the free traction condition on $x^3 \pm h/2$, in addition, one assumes (see Fig. 1)

$$f(h_{<1>}) = f(h_{<2m+1>}) = 0. \tag{4}$$

As concerns $F_\omega\left(\equiv F_\omega\left(x^\lambda\right)\right)$, these are yet unknown functions determining the shape of variation of $\sigma^{\alpha 3}$ in the surfaces parallel to the mid-surface; $B_{<k>}^\alpha\left(\equiv B_{<k>}^\alpha\left(x^\omega\right)\right)$ are functions to be determined upon fulfilling the ICSS, namely

$$S_{<k>}^{\alpha 3}\left(x^3 = h_{<k>}\right) = S_{<k-1>}^{\alpha 3}\left(x^3 = h_{<k>}\right). \tag{5}$$

Following further the procedure outlined in [8], with the help of Eqs. (3) and (5) it can readily be shown that the variation of transverse shear stresses assumes the form

$$S_{<k>}^{\alpha 3}(x^\lambda, x^3) = \left[E_{<k>}^{\alpha 3 \omega 3} f(x^3) + A_{<k>}^{\alpha 3 \omega 3}\right] F_\omega(x^\lambda). \tag{6}$$

In Eqs. (5) and (6) $S^{\alpha 3}$ denote the transverse shear components of the second Piola-Kirchhoff stress tensor S^{ij} while

$$A^{\alpha 3\omega 3}_{<k>} = -\sum_{i=2}^{k} f(h_i)\left[E^{\alpha 3\omega 3}_{<i>} - E^{\alpha 3\omega 3}_{<i-1>}\right]. \quad (7)$$

As shown in Ref. 8 and easily to be inferred from (7), in the case of mild variations of transverse shear moduli, implying $E^{\alpha 3\omega 3}_{<i>} \approx E^{\alpha 3\omega 3}_{<i-1>}$ and hence $A^{\alpha 3\omega 3}_{<i>} \longrightarrow 0$, fulfillment of the ICSS becomes quite redundant. As a result, fulfillment of the static continuity condition has to be enforced whenever the materials of the laminae exhibit significant jumps in transverse shear moduli from layer to layer.

Representation of Tangential Displacement in the Thickness Direction

Assuming that the structure features a stress-free initial geometric imperfection $\overset{\circ}{V}_3\left(x^\omega, x^3\right)\left(\equiv \overset{\circ}{v}_3\left(x^\omega\right)\right)$, considered to be positive downwards, and adopting the concept of small strains and moderately small rotations (Ref. [23]), the 3-D strain-displacement relationship in Lagrangian description is:

$$2e_{ij} = V_{i\|j} + V_{j\|i} + V_{3\|i}V_{3\|j} + V_{3\|i}\overset{\circ}{V}_{3\|j} + \overset{\circ}{V}_{3\|i}V_{3\|j}, \quad (8)$$

where $V_i\left(\equiv V_i\left(x^\omega, x^3\right)\right)$ denote the 3-D displacement components.

In Eq. (8), $(\cdot)_{i\|j}$ stands for the covariant derivative with respect to the metric of the 3-D space.

Postulating that

$$V_3\left(x^\omega, x^3\right) = v_3\left(x^\omega\right), \quad (9)$$

from (8) one can extract the 3-D expression of transverse shear strains expressed in terms of displacement components as

$$2e_{\lambda 3} = V_{\lambda\|3} + V_{3\|\lambda}. \quad (10)$$

Employment in (10) of the relationships connecting covariant derivatives of space and surface tensors specialized for shallow shell theory (see Refs. 19), of constitutive equations for $e^{<k>}_{\lambda 3}$

$$e^{<k>}_{\lambda 3} = 2F^{<k>}_{\lambda 3\mu 3}S^{\mu 3}_{<k>}, \quad (11)$$

as well as of Eq. (6), yields $V^{<k>}_{\lambda,3}$

$$V^{<k>}_{\lambda,3} = 4F^{<k>}_{\lambda 3\mu 3}\left[E^{\mu 3\gamma 3}_{<k>}f(x^3) + A^{\mu 3\gamma 3}_{<k>}\right]F_\gamma - V^{<k>}_{3,\lambda} - b_{\lambda\nu}V^{\nu}_{<k>}. \quad (12)$$

In Eq. (12), $F^{<k>}_{\lambda 3\mu 3}$ denotes the compliance components of $E^{\lambda 3\omega 3}_{<k>}$, fulfilling $E^{\lambda 3\omega 3}_{<k>}F^{<k>}_{\lambda 3\beta 3} = \delta^\omega_\beta/4$.

Integration of (12) in the interval $[0, x^3]$ and employment of (9) yields:

$$V^{<k>}_\lambda = \overline{V}^{<k>}_\lambda - x^3 v_{3|\lambda} + F_\gamma\left[\delta^\gamma_\lambda J_o(x^3) + 4x^3F^{<k>}_{\lambda 3\mu 3}A^{\mu 3\gamma 3}_{<k>}\right]. \quad (13)$$

In Eq. (13), $\overline{V}^{<k>}_\lambda\left(\equiv \overline{V}^{<k>}_\lambda\left(x^\omega\right)\right)$ are arbitrary functions of integration whereas

$$J_o\left(x^3\right) = \int_o^{x^3} f(x^3)dx^3. \quad (14)$$

Upon fulfilling the *kinematic* interlaminae continuity conditions, from Eq. (13) one obtains

$$\overline{V}^{<k>}_\lambda = v_\lambda - 4^{<k>}\Omega^\gamma_{\cdot\lambda}F_\gamma sgnx^3, \quad (k = 1, 2 \ldots m) \quad (15)$$

where $v_\lambda\left(\equiv v_\lambda\left(x^\omega\right)\right)$ denotes the tangential displacements of the mid-surface of the laminate, $sgnx^3(= 1$ for $x^3 > 0$ and $= -1$ for $x^3 < 0)$ denotes the signum distribution, while

$$^{<k>}\Omega^\gamma_{\cdot\lambda} = \sum_{i=1}^{k} h_{<i>}\left(F^{<i>}_{\lambda 3\mu 3}A^{\mu 3\gamma 3}_{<i>} - F^{<i-1>}_{\lambda 3\mu 3}A^{\mu 3\gamma 3}_{<i-1>}\right]. \quad (16)$$

Furthermore, it may readily be shown that

$$^{<k>}\Omega^\gamma_{\cdot\lambda} = {}^{<2m+2-k>}\Omega^\gamma_{\cdot\lambda} \text{ and } {}^{<m+1>}\Omega^\gamma_{\cdot\lambda} = 0. \quad (17)$$

Equation (13) reveals that in the context of this theory the tangential displacements assume a non-linear variation in the thickness direction.

Representation of Tangential Strain Components in the Thickness Direction

With the help of Eqs. (13) nad (15) and after invoking the relationship between covariant derivatives of three-dimensional and surface tensors, from Eqs. (8) one obtains

$$\begin{aligned} ^{<k>}e_{\alpha\beta} = &- x^3 v_{3|\alpha\beta} + \frac{1}{2}J_o\left(x^3\right)\left(F_{\alpha|\beta} + F_{\beta|\alpha}\right) \\ &+ 2x^3\left(F^{<k>}_{\alpha 3\mu 3}A^{\mu 3\gamma 3}_{<k>}F_{\gamma|\beta} + F^{<k>}_{\beta 3\mu 3}A^{\mu 3\gamma 3}_{<k>}F_\sigma\right) \\ &- 2\left({}^{<k>}\Omega^\gamma_{\cdot\alpha}F_{\gamma|\beta} + {}^{<k>}\Omega^\gamma_{\cdot\beta}F_{\gamma|\alpha}\right)sgnx^3 \\ &+ \frac{1}{2}\left(v_{\alpha|\beta} + v_{\beta|\alpha} - 2b_{\alpha\beta}v_3\right). \end{aligned} \quad (18)$$

Equation (18) reveals that the tangential strain components feature a variation through the thickness similar to that of tangential displacement components, Eq. (13)

Constitutive Equations

It is well known (e.g. see Ref. 24) that the 3-D elasticity theory implying small strains but large displacement gradients can be described by linear constitutive equations relating second Piola-Kirchhoff stress tensor with Lagrangian strain tensor.

As a result, using the usual procedure of postulating that transverse normal stress component S^{33} is in constitutive equations negligibly small compared with the other stresses, followed by the elimination of the transverse normal strain component e_{33}, for a material featuring monoclinic symmetry properties the 3-D constitutive equations are

$$\begin{aligned} S^{\alpha\beta} &= \tilde{E}^{\alpha\beta\omega\rho} e_{\omega\rho}, \\ S^{\alpha 3} &= 2E^{\alpha 3\omega 3} e_{\omega 3}, \end{aligned} \qquad (19a,b)$$

where

$$\tilde{E}^{\alpha\beta\omega\rho} = E^{\alpha\beta\omega\rho} - \frac{E^{\alpha\beta 33} E^{33\omega\rho}}{E^{3333}}. \qquad (20)$$

Further, use in conjunction with (19), (6) and (8) of expressions defining, in the context of the shallow shell theory, the stress resultanta $N^{\alpha\beta}$ and $Q^{\alpha 3}$, and the stress couples $M^{\alpha\beta}$

$$\left\{N^{\alpha\beta}, M^{\alpha\beta}\right\} = 2\int_o^{h_{<m+1>}} S^{\alpha\beta}_{<m+1>}\left(1, x^3\right) dx^3$$

$$+2\sum_{r=1}^{m}\int_{h_{<r+1>}}^{h_{<r>}} S^{\alpha\beta}_{<r>}\left(1, x^3\right) dx^3, \qquad (21a)$$

$$Q^{\alpha 3} = 2\int_o^{h_{<m+1>}} S^{\alpha 3}_{<m+1>} dx^3$$

$$+2\sum_{r=1}^{m}\int_{h_{<r+1>}}^{h_{<r>}} S^{\alpha 3}_{<r>} dx^3, \qquad (21b)$$

results in the 2-D constitutive equations which are not displayed here.

Equations of Equilibrium

The previously displayed kinematic equations contain five unknown functions, namely kinematic $v_\alpha(x^\omega)$, $v_3(x^\omega)$ and $F_\alpha(x^\omega)$. As a result, in order to generate the governing equations expressed in terms of these functions, five 2-D equations of equilibrium are needed.

They are obtained by taking various moments of the equations of equilibrium of the 3-D non-linear elasticity theory

$$\left[S^{jr}\left(\delta^i_r + V^i\|_r + \overset{\circ}{V}{}^i\|_r\right)\right]\Big\|_j = 0. \qquad (22)$$

Employment in Eqs. (22) of the approximation proper to the SST followed by consideration of moments of order zero and one of the equations corresponding to $i = 1, 2$ and of moment of order zero of the equation corresponding to $i = 3$ results, with the help of (9) in the 2-D equations of equilibrium:

$$N^{\alpha\beta}|_\beta = 0; \quad M^{\alpha\beta}|_\beta - Q^{\alpha 3} = 0,$$

$$b_{\rho\alpha}N^{\alpha\rho} + N^{\alpha\rho}\left(v_{3,\beta} + \overset{\circ}{v}_{3,\beta}\right)|_\alpha + Q^{\alpha 3}|_\alpha + p_3 = 0, \qquad (23a-c)$$

where $p_3\,(\equiv p_3\,(x^\omega))$ denotes the distributed transversal load.

Upon expressing $N^{\alpha\beta}$ in terms of the Airy's potential function $\Psi(\equiv \Psi(x^\omega)$ as

$$N^{\alpha\beta} = c^{\alpha\omega}c^{\beta\rho}\Psi|_{\omega\rho}, \qquad (24)$$

where $c^{\alpha\beta}$ denotes the 2-D permutation symbol, equation (23a) can be identically satisfied. In this case, the compatibility equation associated with the membrane strains $\varepsilon_{\alpha\beta}$ has to be included as a primary equation of the nonlinear boundary-value problem. It is

$$c^{\alpha\pi}c^{\beta\lambda}\left[\varepsilon_{\alpha\beta|\pi\lambda} + \frac{1}{2}v_{3|\alpha\rho}v_{3|\lambda\pi} + \frac{1}{2}\overset{\circ}{v}_3|_{\pi\lambda}v_{3|\alpha\beta}\right.$$

$$\left.+\frac{1}{2}v_{3|\pi\lambda}\overset{\circ}{v}_{3|\alpha\beta} + b_{\alpha\beta}v_{3|\pi\lambda}\right] = 0. \qquad (25)$$

Governing Equation System

For the problem to be studied in the present paper, a most convenient representation of governing equations is in a form representing the extended counterpart of the classical von Kármán-Mushtari-Marguerre large deflection shell theory. To this end and in order to simplify the problem without impairing upon the generality of the conclusions, a special type of anisotropy of the constituent materials will be considered. This anisotropy is of a transversely-isotropic type, where the surface of isotropy is parallel at each point to the mid-surface σ.

For such a material, the expressions of the 3-D elasticity moduli are presented in Ref. 22. The ratio E/G' constitutes a measure of the transverse shear flexibility of the material. Adoption of Love-Kirchhoff shell model requires that $E/G' \longrightarrow 0$, this reverting to the conclusion that in the context of the classical shell model the constituent materials feature an infinite stiffness in transverse shear (i.e. that $G' \longrightarrow \infty$).

Following the procedure developed in a number of previous papers [18,19] and in the monograph [22], upon expressing $F^\alpha(x^\omega)$ in terms of a new potential function $\phi(x^\omega)$ as

$$\mathcal{K}F^\alpha = -c^{\omega\alpha}\phi|_\omega - Dv_3|^{\alpha\beta}_\beta + \frac{1}{\mathcal{K}}\left(\mathcal{T} + \mathcal{L} + \mathcal{S}\right)p_3|^\alpha$$

$$-\left[N^{\omega\rho}\left(v_{3|\omega\rho} + \overset{\circ}{v}_{3|\omega\rho}\right)\right]|^\alpha - b_{\rho\omega}N^{\omega\rho}|^\alpha, \qquad (26)$$

and using the representation for $N^{\alpha\beta}$ given by (24), two governing equations are obtained as:

$$Dv_3|^{\alpha\beta}_{\alpha\beta} - c^{\omega\alpha}c^{\rho\beta}\{b_\rho\omega\Psi_{|\alpha\beta} + (v_{3|\omega\rho} + \overset{\circ}{v}_{3|\omega\rho})\Psi_{|\alpha\beta} - \frac{\mathcal{T}+\mathcal{L}+\mathcal{S}}{\mathcal{K}}(b_{\rho\omega}\Psi_{|\alpha\beta} + \Psi_{|\alpha\beta}(v_{3|\rho\omega} + \overset{\circ}{v}_{3|\rho\omega}))|^{\sigma}_{\sigma}\} - (p_3 - \frac{\mathcal{T}+\mathcal{L}+\mathcal{S}}{\mathcal{K}}p_3|^{\alpha}_{\alpha}) = 0, \tag{27a}$$

and

$$\phi - \frac{\mathcal{T}_1+\mathcal{L}_1+\mathcal{S}_1}{\mathcal{K}}\phi|^{\alpha}_{\alpha} = 0. \tag{27b}$$

In addition, the compatibility equation (25) expressed in terms of Ψ and v_3 becomes:

$$\left(\tilde{b}+\tilde{c}\right)\Psi|^{\lambda\pi}_{\lambda\pi} + \frac{1}{2}\left(v_3|^{\rho}_{\rho}v_3|^{\lambda}_{\lambda} - v_3|^{\lambda}_{\rho}v_3|^{\rho}_{\lambda}\right) + \left(\overset{\circ}{v}_3|^{\pi}_{\pi}v_3|^{\alpha}_{\alpha} - \overset{\circ}{v}_3|^{\pi}_{\alpha}v_3|^{\alpha}_{\pi}\right) + \left(2Hv_3|^{\pi}_{\pi} - b^{\beta}_{\lambda}v_3|^{\lambda}_{\beta}\right) = 0. \tag{28}$$

In these equations $\mathcal{T}(\equiv \mathcal{T}_1+\mathcal{T}_2)$, $\mathcal{L}(\equiv \mathcal{L}_1+\mathcal{L}_2)$, $\mathcal{S}(\equiv \mathcal{S}_1+\mathcal{S}_2)$ and $\mathcal{K}$ are stiffness quantities whose expressions are recorded in Ref. 8; $(\cdot)|^{\alpha}_{\alpha}$ and $(\cdot)|^{\alpha\beta}_{\alpha\beta}$ denote the 2-D Laplace and biharmonic operators, respectively; $2H\left(\equiv b_{\alpha\beta}a^{\alpha\beta} = (1/R_1 + 1/R_2)\right)$ denotes the mean curvature of σ where R_α denote the principal radii of curvature of σ.

It should be mentioned that the linear Eq. (27b) defines the boundary layer effect. Its solution is characterized by a rapid decay when proceeding from the edges towards the interior of the shell. Although uncoupled in the governing equations, the unknown function ϕ remains coupled with the other two functions, Ψ and v_3, in the equations expressing the boundary conditions (in number of five at each edge).

As was shown previously [18,19], *for simply supported boundaries*, the function ϕ could be rendered decoupled in the boundary condition, and as a result, the boundary layer equation (27b) in conjunction with the associated boundary conditions admits the trivial solution $\phi = 0$. In such a case Eq. (27b) can be exactly discarded and, as a result, the order of governing equations reduces from ten to eight, implying a reduction of the number of boundary conditions from five to four.

Postbuckling of Flat and Doubly Curved Shallow Panels with Rectangular Planform

The postbuckling behavior of simply-supported doubly curved panels with rectangular planform on P will be analyzed. We will refer the points of σ to a Cartesian orthogonal system of coordinates assumed to be parallel to the panel edges. We consider that the panel is subjected to a system of uniform in-plane biaxial compressive edge loads $\tilde{L}_{11}$ and $\tilde{L}_{22}$ whose ratio is $L_R\left(\equiv \tilde{L}_{22}/\tilde{L}_{11}\right)$.

Depending upon the **in-plane** behavior at the edges, two cases, labelled as Case A) and Case B) will be considered:

Case A) The edges are simply supported and freely movable in the direction normal to the unloaded edges in the plane tangent to the surface at the panel edges.

Case B) The edges are simply supported. Uniaxial edge loads are acting in the direction of the x_1-coordinate. The edges $x_1 = 0, \ell_1$ are considered freely movable, the remaining two edges being unloaded, their in-plane motion in direction normal to the edges being prevented. In the present case edges $x_2 = 0,\ \ell_2$ are referred to as immovable.

It can be shown that the representations for v_3 and $\overset{\circ}{v}_3$

$$\left\{\begin{matrix} v_3\,(x_\alpha) \\ \overset{\circ}{v}_3 \end{matrix}\right\} = \left\{\begin{matrix} f_{mn} \\ \overset{\circ}{f}_{mn} \end{matrix}\right\} \sin\lambda_m x_1 \sin\mu_n x_2, \tag{29a}$$

where

$$\lambda_m \equiv m\pi/\ell_1,\ \mu_n = n\pi/\ell_2, \qquad (m,n = 1,2\ldots) \tag{29b}$$

fulfill exactly the **out-of-plane** BC's. The **in-plane** BCs are satisfied on an average. To this end, the potential function Ψ is represented as:

$$\Psi(x_a) = \Psi_1(x_\alpha) - \frac{1}{2}\left((x_2)^2\tilde{L}_{11} + (x_1)^2\tilde{L}_{22}\right). \tag{30}$$

Here $\Psi_1\,(\equiv \Psi_1\,(x_\alpha))$ is a particular solution of Eq. (28) (determined in conjunction with (29)) while $\tilde{L}_{11}$ and $\tilde{L}_{22}$ denote the normal edge loads (considered positive in compression).

In the case of the panel loaded in the direction of the x_1-coordinate only, the remaining edges being unloaded and immovable, (that is of the Case B), the condition for the immovable edges $x_2 = 0, \ell_2$ may be expressed in an average sense (see [22]),

$$\int_0^{\ell_1}\int_0^{\ell_2} v_{2,2}dx_1.dx_2 = 0. \tag{31}$$

This equation provides the corresponding $\tilde{L}_{22}$ for which the edges $x_2 = 0, \ell_2$ remain immovable. Galerkin's procedure applied to the Eq. (27a) yields the equation governing the postbuckling behavior of laminated composite curved panels subjected to biaxial compressive edge loads and a pressure field.

This equation as well as the expression of $\Psi_1(x_\alpha)$ are not displayed here.

The obtained equation enables ones to illustrate in the plane ($\tilde{L}_{11}$ vs. $\delta+\overset{\circ}{\delta}$ or $\hat{p}$ vs. $\delta+\overset{\circ}{\delta}$) the postbuckling behavior of curved and flat panels. However, another representation of the postbuckling behavior enabling one to correlate the theoretical findings with the experimental ones is established in the plane ($\tilde{L}_{11}$ vs. Δ_1), where Δ_1 denotes the average end-shortening in the direction of the coordinate x_1.

This is defined as

$$\Delta_1 = -\frac{1}{\ell_1\ell_2}\int_0^{\ell_1}\int_0^{\ell_2} v_{1,1}dx_1dx_2. \qquad (32)$$

The explicit expression of this quantity is not displayed here.

The goal of this paper is to ascertain the effects brought by the non-fulfillment of transverse-shear stress continuity requirement upon the postbuckling response of a three-layer sandwich-type flat/curved panel compressed by a system of compressive edge loads and subjected to a lateral pressure $p_3(x_\alpha)$.

In the numerical illustrations $\delta\,(\equiv f_{11}/h)$ and $\delta_o\left(\equiv \overset{\circ}{f}_{11}/h\right)$ denote the normalized transverse deflection and initial geometric imperfection in the first mode associated with the central point of the panel. The dimensionless pressure coefficient $\hat{p}\left(\equiv p_3\left(\ell_1/2,\ell_2/2\right)\ell_1^4/(Dh)\right)$ is evaluated at the center of the panel where its maximum occurs.

Numerical Illustrations and Discussion

The numerical illustrations include comparisons of the postbuckling response obtained in the context of Models I and II. Throughout these numerical illustrations it was considered a square ($\ell_1 = \ell_2 = \ell$) projection of the panel on the plane P and, unless otherwise stated, it was assumed that the thickness of the core layer is twice as thick as that of the face layer (i.e. $t_c = 2t_f$) and that the panel is uniaxially compressed. Herein indices f and c denotes the affiliation of the respective quantity to the face and core layer, respectively.

In the absence of any specification about the character of in-plane boundary conditions one should consider the edges freely-movable (i.e., Case A). The postbuckling response of geometrically perfect/imperfect three-layer flat panels compressed by uniaxial/biaxial edge loads predicted in the context of Models I and II are displayed in Figs. 2 and 3.

Notice that $L_R\left(\equiv \tilde{L}_{22}/\tilde{L}_{11}\right) = 0$, corresponds to a panel uniaxially compressed by $\tilde{L}_{11}$. The results reveal that with the relative increase of the transverse shear flexibility of the core layer material, from the slight underestimation of the load carrying capacity (LCC), Model I starts to slightly overestimate the LCC. The results also reveal that this trend occurs for both the perfect and geometrically imperfect panels.

Figures 4 and 5 enforce and extend this conclusion to the case of a circular cylindrical panel. The results obtained for this case displayed both in the plane $\left(\tilde{L}_{11},\delta+\delta_o\right)$ and $\left(\tilde{L}_{11},\Delta_1\right)$ reveal that, depending of the relative degree of transverse shear flexibility of the core layer material, in the deep postbuckling range the degree of underestimation/overestimation of the LCC is even exacerbated.

Figures 6a and 6b obtained for the case of circular cylindrical sandwich type panel bring into evidence the effect played on the postbuckling response by the ratio t_c/t_f, where t_c and t_f denote the thicknesses of the core and of face layers, respectively.

The results reveal that in the case of the core material featuring a large transverse shear flexibility, the decrease/increase of its thickness while maintaining the total thickness as a constant valued quantity, results in an increase/decrease of the LCC. At the same time the results also show that until a certain value of the thickness parameter t_c/t_f, Model I underpredicts the LCC, and with the increase of that parameter beyond a certain critical value (in the present case that specific value corresponds to $t_c/t_f = 10$), the opposite trend becomes valid. Moreover, it is seen that with the increase of the core thickness in the detriment of the thickness of faces, an increase of the intensity of the snap-through bucklings is experienced.

Figures 7 and 8 obtained for a slightly geometrically imperfect circular cylindrical panel highlight the effect played by the ratio of transverse shear moduli G_c'/G_f' and implicitely by the relative transverse shear flexibility characteristics of face and core layers.

Figure 7 reveals that when the core layer features a rather moderate transverse shear flexibility ($E_c/G_c' = 10$), Model I features a weak sensitivity to the variation of the E_f/G_f'.

The same figure also reveals that for transverse shear flexibilities of the faces larger than those of the core, a deterioration of the LCC is experienced and that Model I provides an overestimation of, load carrying capacity predictions. Moreover, the increase of transverse shear flexibility of the faces is accompanied by a deterioration of the LCC and by an increase of the intensity of the snap-through buckling. However, the opposite trend appears to be valid when the core layer material features higher flexibilities in transverse shear than those of the faces.

Figures 9a and 9b depict in the planes $(\tilde{L}_{11},\delta)$ and $(\tilde{L}_{11},\Delta_1)$, respectively, the postbuckling response of

a geometrically perfect circular cylindrical three-layer panel subjected to a pressure field of intensity $\hat{p}$ and to uniform compressive loads applied on its curved edges. It is also supposed that the straight edges can be freely moveable or immoveable.

The depicted results reveal that for low intensities of transverse load the immoveability of straight edges appears to be beneficial from the LCC standpoint and that the predictions obtained within the Models I and II coincide. However, with the increase of the transverse load, the immoveability of those edges yields a deterioration of the LCC in the sense that instead of getting a monotonous increase of the LCC (trend valid in the case of moveable straight edges), in the case of its immoveable edge counterpart, a relatively large limit load is featured followed by a strong snap-through buckling.

The results also reveal that in this case Model I underestimates the LCC as compared to Model II.

Finally, Fig. 10a and 10b compare the post-buckling predictions for an initially imperfect circular cylindrical sandwich panel obtained in the context of the Models I and II, of the classical shell theory, and of the first order transverse shear deformation theory (FSDT), this one extracted from Model I (see Refs. [18,19]).

In addition to the well-known fact that the classical shell theory grossely overestimates the LCC, the results reveal that in the case of larger curvature ratios, (as is the case analyzed here) the difference between the postbuckling predictions provided by the Models I and II increase. It should also be noticed that the result outlined in a number of papers based on Model I (see Refs. [18,19]) according to which the postbuckling predictions based on HSDT and FSDT (with the shear correction factor $K^2 = 2/3$) are in better agreement than in the case of the consideration of $K^2 = 5/6$, should be changed when dealing with the Model II. In this latter case, the predictions provided by the FSDT with $K^2 = 5/6$ are closer to the ones provided by the HSDT associated with Model II.

Conclusions

A parametric study intended to bring new elements on the problem of implications on the postbuckling response of flat/curved laminated composite and sandwich panels induced by the violation of the ICSS was undertaken.

In order to accomplish such a study, a simple geometrically non-linear model of laminated shells (referred to as Model II), fulfilling both the kinematic and static interlaminae continuity conditions as well as the ones at the external boundary surfaces of the shell was devised and used.

As was diagramatically shown, depending upon the relative transverse shear flexibility featured by the materials of the core and face layers, Model I (which violates the ICSS requirement) can provide under/overestimations of the load carrying capacity of the panel. Depending upon the degree of jump of transverse shear flexibilities and of the thickness of layers featuring larger transverse shear flexibility ratios, the resulting implications can be extremely significant

It was also numerically verified what was conjectured in (Refs. 13,15), namely that the Model II provides results in better agreement with FSDT when $K^2 = 5/6$ is considered. Certainly, there are still many other cases in which Model II should be used when more accurate predictions of the LCC are needed. Nevertheless, in studies involving determination of failure conditions in the postbuckling range of sandwich structures, wherein prediction of *local* response characteristics is of prime importance, Model II turns out to be the only structural model able to provide reliable results in the matter.

Acknowledgement

Two authors of this paper (M. DiS. and U. I.) would like to thank Consiglio Nazionale delle Ricerche for the support of this research.

References

1. Kapania, R. K., "A Review on the Analysis of Laminated Shells," *Journal Pressure Vessel Tech*, ASME, 111. May 1989, pp. 88-96.

2. Noor, A. K. and Burton, W. S., "Assessment of Computational Models for Multilayered Composite Shells," *Appl. Mech. Rev.*, **43**, 4, April, pp. 67-97, 1990.

3. Di Sciuva, M., "Bending Vibration and Buckling of Simply-Supported Thick Multilayered Orthotropic Plates: An Evaluation of a New Displacement Model," *Journal of Sound and Vibration*, Vol. 105, pp. 425-442, 1986.

4. Di Sciuva, M. and Carrera, E., "Elastodynamic Behaviour of Relatively Thick, Symmetrically Laminated Anisotropic Circular Cylindrical Shells," *Journal Appl. Mechanics*, Trans. ASME, **59**, pp. 222-224, 1992.

5. Toledano, A. and Murakami, H., "A High-Order Laminated Plate Theory with Improved In-Plane Responses," *International J. Solids and Structures*, (23), 1, pp. 111-131, 1987.

6. Timarci, T. and Soldatos, K.S., Influence of Boundary Conditions on Vibrations of Cross-Ply Laminated Cylindrical Shells on the Basis of a

Unified Shear Deformable Shell Theory, *Journal of Sound and Vibration* (in press).

7. He, L. H., "A Linear Theory of Laminated Shells Accounting for Continuity of Displacement and Transverse Shear Stresseds at Layer Interfaces," *International J. Solids Structures*, **31** 5, pp. 613-627, 1994.

8. Librescu, L. and Lin, W., "Two Models of Shear Deformable Laminated Plates and Shells and Their Use in Prediction of Global Response Behavior", *European Journal of Mechanics/Solids* (in press).

9. Di Sciuva, M., "A Refined Transverse Shear Deformation Theory for Multilayered Anisotropic Plates," *Atti Academia dlle Scienze di Torino Classe de Scienze Fisiche Matematiche e Naturali*, Vol. 118, pp. 279-295, 1984.

10. Di Sciuva, M., "Further Refinement in the Transverse Shear Deformation Theory for Multilayered Composite Plates," *Atti Accademia delle Scienze di Torino-Classe di Scienze Fisiche, Mathematiche e Naturali*, Vol. 124, Fasc, 5-6, pp. 248-267, 1990.

11. Di Sciuva, M., "Multilayered Anisotropic Plate Models with Continuous Interlaminar Stresses," *Composite Structures*, **22**, pp. 149-164, 1992.

12. Ambartsumian, S. A., "Theory of Anisotropic Plates: Strength, Stability, and Vibration," (in Russian), Nauka, Moskow, 1987.

13. Schmidt, R. and Librescu, L., "Further Results Considering the Refined Theory of Anisotorpic Laminated Composite Plates," *Journal of Engineering Mathematics*, **28**, pp. 407-425, 1994.

14. Di Sciuva, M., "An Improved Shear-Deformation Theory for Moderately Thick Multilayered Anisotropic Shells and Plates," *Journal Applied Mechanics*, Trans. ASME, **54**, 3, pp. 589-596, 1987.

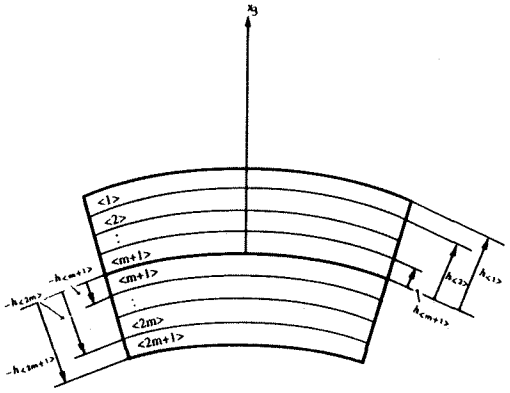

Fig. 1 Geometry of the shell cross-section

15. Librescu, L. and Schmidt, R., "Substantiation of a Shear-Deformable Theory of Anisotropic Composite Laminated Shells Accounting for the Interlaminae Continuity Conditions", *International J. of Engineering Science*, **29**, pp. 669-683, 1991.

16. Pai, P.F. and Nayfeh, A.H., "A Unified Nonlinear Formulation for Plate and Shell Theories", *Nonlinear Dynamics*, **6**, pp. 459-500, 1994.

17. He, L-H., "Non-Linear Theory of Laminated Shells Accounting for Continujity Conditions of Displacementse and Tractions at Layer Interfaces," *International J. Mechanical Sciences*, **37**, 2, pp. 161-173, 1995.

18. Librescu, L. and Stein, M., "Postbuckling Behavior of Shear Deformable Composite Flat Panels Taking Into Account Geometrical Imperfections," *AIAA Journal*, Vol. 30, pp. 1352-1360, May 1992.

19. Librescu, L. and Chang. M.-Y., "Post-Buckling and Imperfection Sensitivity of Shear Deformable Composite Doubly-Curved Panels," *International J. Solids and Structures*, Vol. 29, No. 9, pp. 1065-1083, 1992.

20. Green, A. E., and Zerna, W., *Theoretical Elasticity*, Oxford: At the Clarendon Press.

21. Naghdi, P. M., "Foundation of Elastic Shell Theory," *Progress of Solid Mechanics*, (Eds. Sneddon, L. N. and Hill, R.), 4. 1. 1963.

22. Librescu, L., *Elastostatics and Kinetics of Anisotropic and Heterogeneous Shell-Type Structures*, Noordhoff Internat. Publ. Netherlands, Leyden, 1975.

23. Librescu, L., "Refined Geometrically Non-Linear Theories of Anisotropic Laminated Shells," *Quarterly Appl. Mathematics*, **45**, pp. 1-22, 1987.

24. Malvern, L. E., *Introduction to the Mechanics of a Continuous Medium*, Prentice-Hall, Englewood Cliffs, 1969.

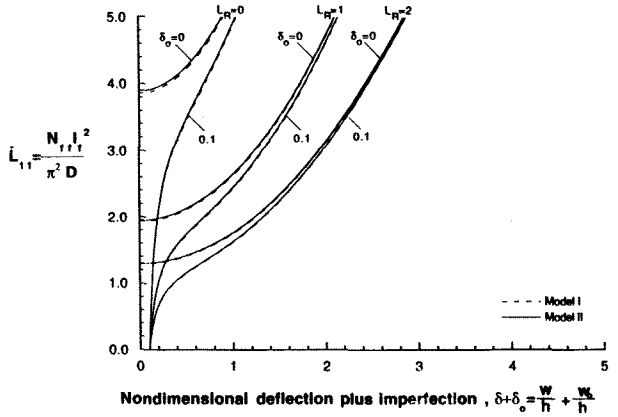

Fig. 2a Comparisons of the postbuckling response of geometrically perfect/imperfect flat panels ($\ell_1/\ell_2 = 1,\ t_c/t_f = 2,\ \ell_1/h = 20,$ $(E/G')_f = 3,\ (E/G')_c = 15,\ E_f = E_c,$ $\nu = \nu' = 0.3$) under uniaxial ($L_R = 0$) and biaxial ($L_R \neq 0$) compressive loads as predicted by Models I and II.

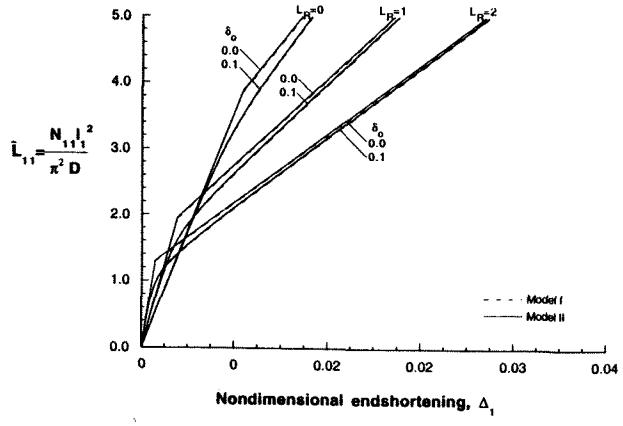

Fig. 2b The counterpart of the case considered in Fig. 2a, depicted in the plane ($\tilde{L}_{11},\ \Delta_1$).

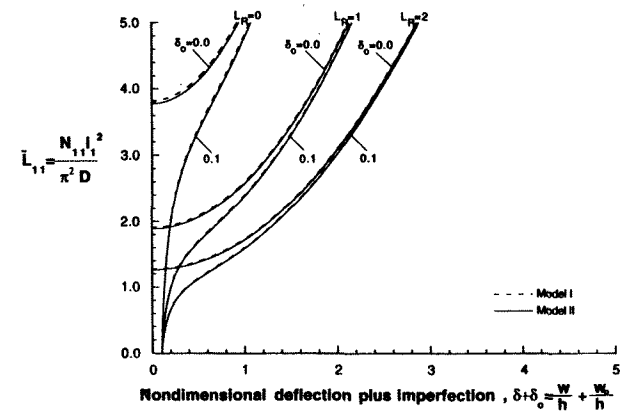

Fig. 3 The counterpart of the case described in Fig. 2 for $(E/G')_c = 60$.

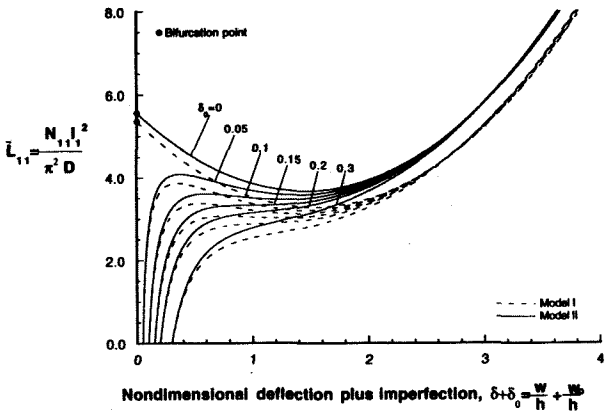

Fig. 4a Comparisons of the postbuckling response of geometrically perfect/imperfect circular panels ($\ell_1/h = 20,\ \ell_1/R_1 = 0,\ \ell_2/R_2$ $= 0.5$), $(E/G')_c = 30$, $(E/G')_f = 10$, E_f/E_c $= 10,\ \nu = \nu' = 0.2$) under uniaxially compressive edge loads as predicted by Models I and II.

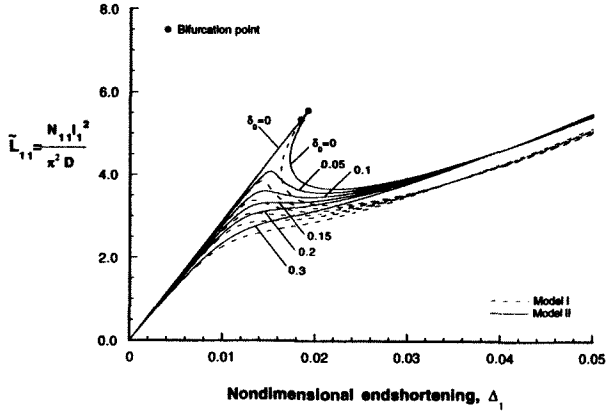

Fig. 4b The counterpart of the case considered in Fig. 4a depicted in the plane ($\tilde{L}_{11}, \Delta_1$).

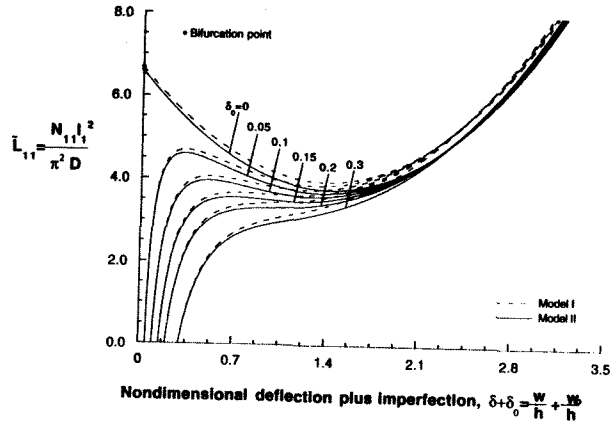

Fig. 5a The counterpart of the case described in Figs. 4 for the case $(E/G')_f = 2,\ (E/G')_c$ $= 60,\ E_f = E_c,\ \nu = \nu' = 0.3$.

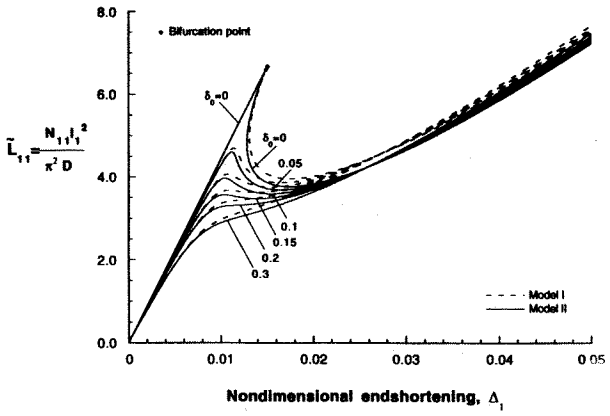

Fig. 5b The counterpart of Fig. 5a depicted in the plane $(\tilde{L}_{11},\ \Delta_1)$.

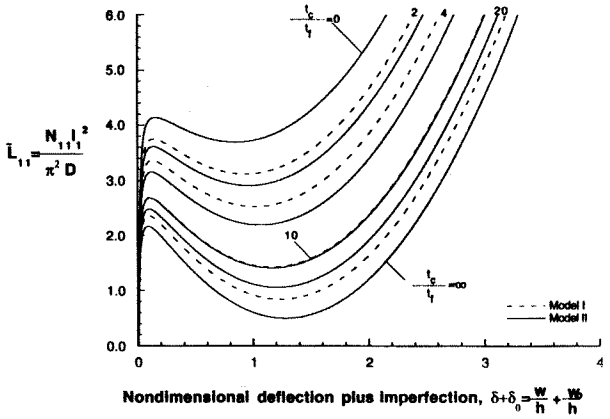

Fig. 6a Influence of the thickness ratio t_c/t_f on the postbuckling response of uniaxially compressed geometrically imperfect ($\delta_0 = 0.01$) circular cylindrical panels ($\ell_1/R_1 = 0, \ell_2/R_2 = 0.6$) of moderate thickness ($\ell_1/h = 10$) characterized by $(E/G')_f = 3$, $(E/G')_c = 60$, $E_f = E_c$, as predicted by Models I and II.

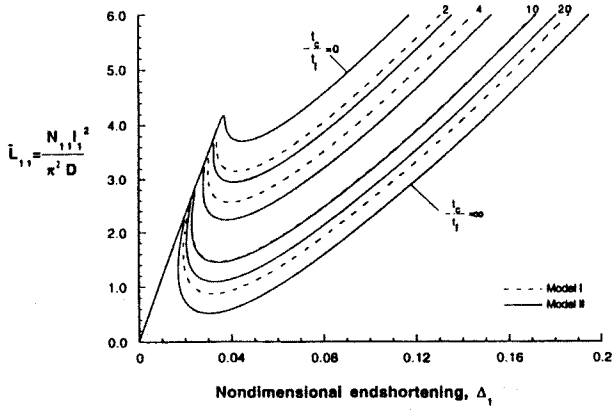

Fig. 6b The counterpart of the case considered in Fig. 6a depicted in the plane $(\tilde{L}_{11}, \Delta_1)$.

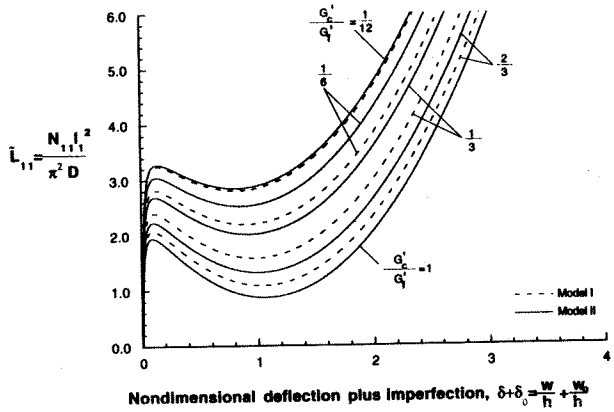

Fig. 7 Influence of the ratio of transverse shear moduli G_c'/G_f' on the postbuckling response of uniaxially compressed geometrically imperfect ($\delta_0 = 0.01$) circular cylindrical panels ($\ell_1/R_1 = 0$, $\ell_2/R_2 = 0.5$) of moderate thickness ($\ell_1/h = 10$), characterized by $(E/G')_c = 60$, $E_f = E_c$, as predicted by Models I and II.

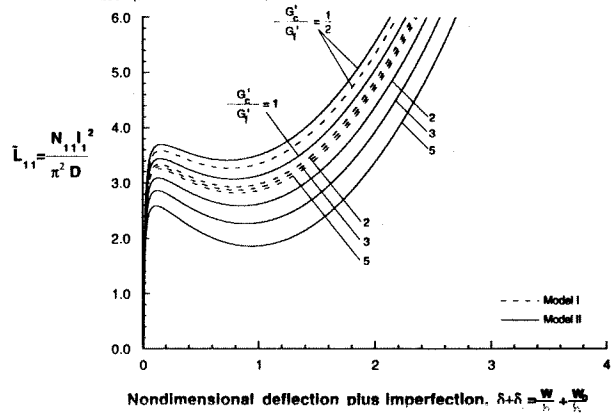

Fig. 8 The counterpart of Fig. 7 for $(E/G')_c = 10$.

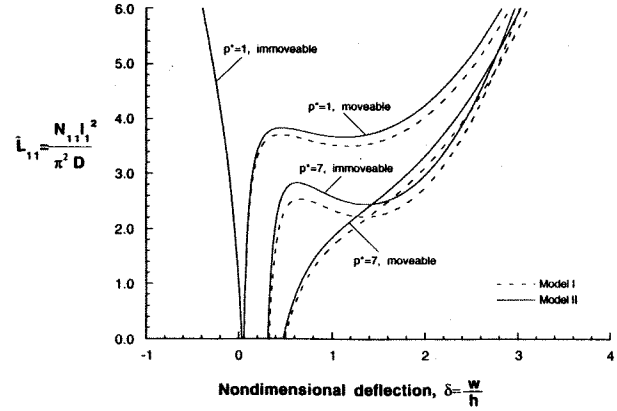

Fig. 9a Influence of the lateral pressure and of the tangential immovability/moveability of straight edges on the postbuckling response of uniaxially compressed geometrically perfect circular cylindrical panels ($\ell_1/h = 30$, $\ell_1/R_1 = 0$, $\ell_2/R_2 = 0.3$, $t_c/t_f = 2$, $(E/G')_f = 3$, $(E/G')_c = 15$, $E_f = E_c$, $\nu = \nu' = 0.3$).

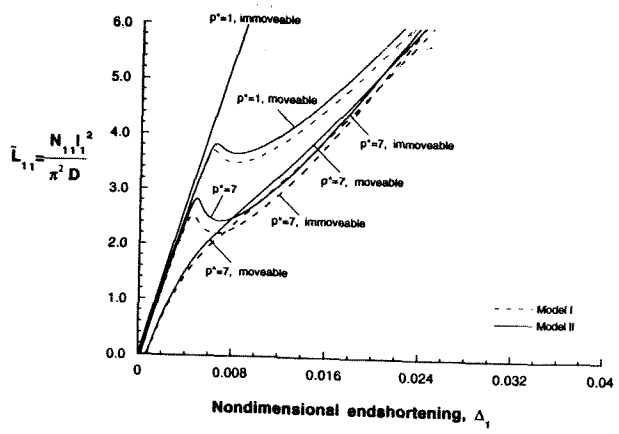

Fig. 9b The counterpart of Fig. 9a depicted in the plane $(\tilde{L}_{11},\ \Delta_1)$.

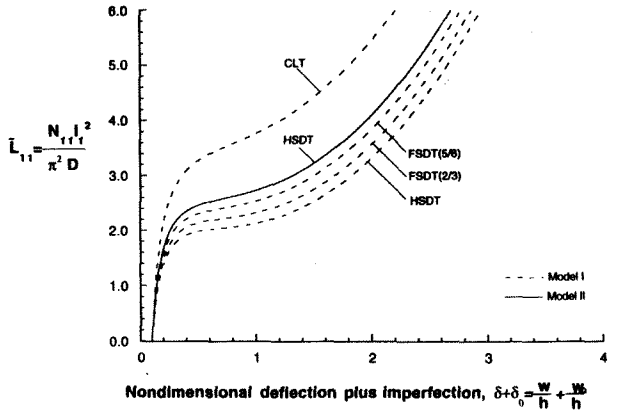

Fig. 10a Influence of the modelling on the post-buckling predictions of geometrically perfect circular cylindrical panels subjected to uniaxial compressive loads ($\ell_1/h = 10$, $\ell_1/R_1 = 0$, $\ell_2/R_2 = 0.5$, $t_c/t_f = 2$, $(E/G')_f = 3$, $(E/G')_c = 60$, $E_c = E_f$. The numbers in brackets denote the values of transverse shear correction factor.

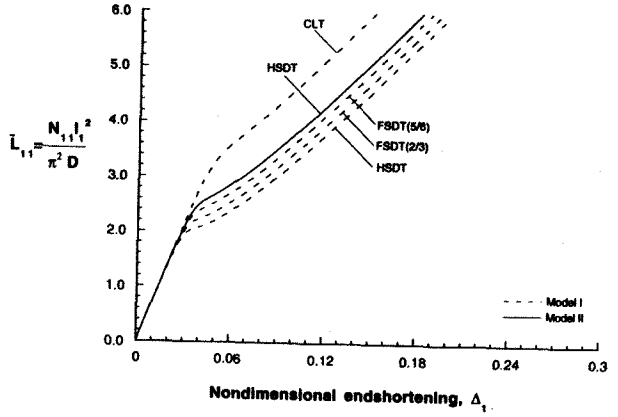

Fig. 10b The counterpart of Fig. 10a in the plane $(\tilde{L}_{11},\ \Delta_1)$.